IOPscience iopscience.iop.org

Home Search Collections Journals About Contact us My IOPscience

Resonance tuning of piezoelectric vibration energy scavenging generators using compressive axial preload

This content has been downloaded from IOPscience. Please scroll down to see the full text.

2006 Smart Mater. Struct. 15 1413

(http://iopscience.iop.org/0964-1726/15/5/030)

View the table of contents for this issue, or go to the journal homepage for more

Download details:

IP Address: 93.180.53.211
This content was downloaded on 05/12/2013 at 11:54

Please note that terms and conditions apply.

INSTITUTE OF PHYSICS PUBLISHING SMART MATERIALS AND STRUCTURES
Smart Mater. Struct. **15** (2006) 1413–1420 doi:10.1088/0964-1726/15/5/030

Resonance tuning of piezoelectric vibration energy scavenging generators using compressive axial preload

Eli S Leland and Paul K Wright

Department of Mechanical Engineering, University of California, Berkeley, Berkeley, CA 94720, USA

E-mail: eli@me.berkeley.edu and pwright@kingkong.me.berkeley.edu

Received 3 February 2006, in final form 28 July 2006
Published 8 September 2006
Online at stacks.iop.org/SMS/15/1413

Abstract
Vibration energy scavenging, harvesting ambient vibrations in structures for conversion into usable electricity, provides a potential power source for emerging technologies including wireless sensor networks. Most vibration energy scavenging devices developed to date operate effectively at a single specific frequency dictated by the device's design. However, for this technology to be commercially viable, vibration energy scavengers that generate usable power across a range of driving frequencies must be developed. This paper details the design and testing of a tunable-resonance vibration energy scavenger which uses the novel approach of axially compressing a piezoelectric bimorph to lower its resonance frequency. It was determined that an axial preload can adjust the resonance frequency of a simply supported bimorph to 24% below its unloaded resonance frequency. The power output to a resistive load was found to be 65–90% of the nominal value at frequencies 19–24% below the unloaded resonance frequency. Prototypes were developed that produced 300–400 μW of power at driving frequencies between 200 and 250 Hz. Additionally, piezoelectric coupling coefficient values were increased using this method, with k_{eff} values rising as much as 25% from 0.37 to 0.46. Device damping increased 67% under preload, from 0.0265 to 0.0445, adversely affecting the power output at lower frequencies. A theoretical model modified to include the effects of preload on damping predicted power output to within 0–30% of values obtained experimentally. Optimal load resistance deviated significantly from theory, and merits further investigation.

1. Introduction

Vibration energy scavengers are devices that convert mechanical energy from vibrations into usable electrical energy. The ongoing development of low-power wireless sensors provides a motivation for vibration energy scavenging. The small form factor and multi-year expected lifetimes of wireless sensor nodes require a compact, 'infinite' power source to supplement or replace existing battery technologies. Solar cells provide one such alternative, but vibration energy scavenging becomes an attractive option in deployment environments where poor lighting conditions exist.

Most vibration energy scavenging devices developed to date are resonant devices whose dominant resonance frequency is determined by the material properties and dimensions of the device's component parts. As such, these devices tend to convert energy most effectively when the frequency of the driving vibration source (typically a vibrating surface or structure upon which the device is mounted) closely matches the fixed resonance frequency of the device. A frequency mismatch of only a few per cent, however, results in a significant decrease in power output. This phenomenon suggests the need for a vibration energy scavenger design whose resonance frequency can be adjusted, or 'tuned,' to

match the driving vibrations across a range of frequencies. This paper details the design, fabrication, and testing of a new type of tunable-resonance vibration energy scavenger that uses the novel approach of applying a compressive axial preload to adjust the resonance frequency of a piezoelectric bimorph.

A variety of designs and applications for vibration energy scavengers have been examined previously. These include designs using cantilever-mounted piezoelectric bimorphs (Glynne-Jones *et al* 2001, Roundy and Wright 2004), electromagnetic devices (Glynne-Jones *et al* 2004), and electrostatic devices (Miyazaki *et al* 2003, Roundy *et al* 2003). Studies have sought to improve the power output of vibration energy scavengers (Baker *et al* 2005, Roundy *et al* 2005). Vibration-powered sensor nodes have also been used to monitor ambient temperature (Leland *et al* 2004) and machine tool condition (James *et al* 2004).

Multiple options are available in designing a tunable-resonance energy scavenger. Roundy and Zhang (2005) examined the possibility of 'actively' tuning a device's resonance characteristics and presented a design that used electrical feedback to alter the resonance frequency of a piezoelectric bimorph. The study presented herein, however, sought to design a device that operated 'passively', which is to say that it could be adjusted periodically to tune its resonance frequency but would require no continuous actuation. Alternatives for a piezoelectric bimorph-based design included adjusting the bimorph's length, adjusting the proof mass mounted on the bimorph, and using axial preloads to alter the bimorph's stiffness. Tensile loads presented potential problems arising from the inherently brittle nature of piezoelectric ceramics. The use of a compressive axial preload was chosen, as it allowed for a straightforward design whose resonance could be easily adjusted. Moreover, previous work by Lesieutre and Davis (1997) showed that compressive axial preloads can increase the coupling coefficient of an electrically driven piezoelectric bimorph.

A novel design for a tunable-resonance vibration energy scavenger was developed and built in this study. This device used a simply supported piezoelectric bimorph as its active element, with a proof mass mounted at the bimorph's center. A variable compressive axial preload was applied to the bimorph, reducing its stiffness and thus the resonance frequency of the device. Experiments examined the effects of compressive axial preload on the vibration energy scavenger's resonance characteristics, piezoelectric device coupling coefficient, damping ratio, and power output.

2. Theoretical background

2.1. Resonance of an unloaded simply supported bimorph

Figure 1 shows a schematic of a simply supported piezoelectric bimorph vibration energy scavenger. The bimorph in this design consists of a brass center shim coated on either side with a layer of lead zirconate titanate (PZT) piezoelectric ceramic.

In the absence of axial preload, the resonance frequency ω_o of the generator is described by

$$\omega_o = \sqrt{\frac{K_o}{m_{eff}}} \tag{1}$$

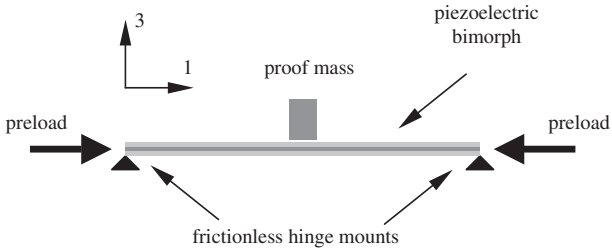

Figure 1. Schematic of a simply supported piezoelectric bimorph vibration energy scavenger.

Table 1. Variable descriptions and their values.

Symbol	Description	Value	Units
m_p	Proof mass	7.1, 12.2	g
b	Bimorph width	12.7	mm
L	Bimorph length	31.7	mm
h_b	Brass shim thickness	0.127	mm
E_b	Brass shim Young's modulus	100	GPa
ρ_b	Brass density	8140	kg m^{-3}
h_p	Piezo layer thickness	0.191	mm
E_p	Piezo Young's modulus	52	GPa
ρ_p	Piezo density	7800	kg m^{-3}
C_b	Bimorph capacitance	15.5	nF
e_{31}	Piezoelectric coefficient	−9.88	C m^{-2}

where K_o is the transverse stiffness of the center of the bimorph, and m_{eff} is the effective mass acting on the center of the beam. The transverse stiffness of a homogeneous simply supported element is given by the Euler–Bernoulli model as

$$K_o = EI\left(\frac{\pi}{L}\right)^4\left(\frac{L}{2}\right) \tag{2}$$

where EI represents the bending stiffness, defined as the product of the Young's modulus and the second moment of area, and L is the length of the bimorph. Table 1 details the names and descriptions of a number of variables used in the following equations. Accounting for the bimorph's multiple layers, the transverse stiffness takes on the more complicated form

$$K_o = b\left(E_b\frac{h_b^3}{12} + 2E_p\left(\frac{h_p^3}{12} + h_p\left(\frac{h_b + h_p}{2}\right)^2\right)\right) \times \left(\frac{\pi}{L}\right)^4\left(\frac{L}{2}\right). \tag{3}$$

The effective mass is equal to the proof mass plus one-half the mass of the bimorph:

$$m_{eff} = m_p + \frac{bL}{2}(\rho_b h + 2\rho_p h_p). \tag{4}$$

2.2. Effects of compressive axial preload on resonance

The new energy scavenger design presented in this study uses a compressive axial preload to alter the resonance frequency of the device. The application of a compressive axial preload destabilizes the simply supported bimorph, effectively

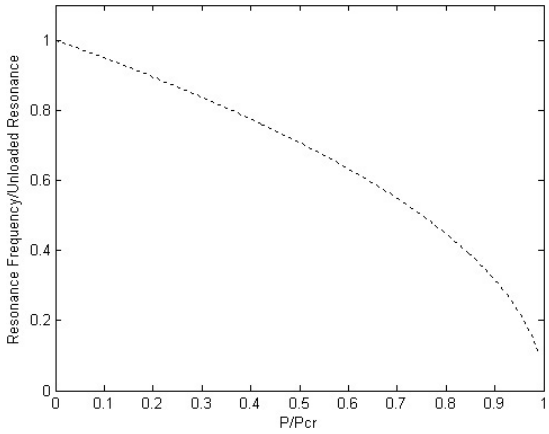

Figure 2. Resonance frequency versus preload, normalized.

reducing its transverse stiffness. The new apparent stiffness K_{app} is defined as

$$K_{app} = K_o - K_d \tag{5}$$

where K_d is the destabilizing stiffness term introduced as a result of the preload. K_d is defined as

$$K_d = P\left(\frac{\pi}{L}\right)^2\left(\frac{L}{2}\right) \tag{6}$$

where P is the value of the compressive axial preload (Lesieutre and Davis 1997). The resonance frequency of the bimorph under preload is thus modified to

$$\omega_o = \sqrt{\frac{K_{app}}{m_{eff}}}. \tag{7}$$

As the preload is increased, the value of K_d increases ultimately to the point where the bimorph's apparent stiffness, and thus its resonance frequency, are equal to zero. The compressive preload at which the bimorph is fully destabilized is equal to the critical buckling load P_{cr}, given by

$$P_{cr} = \frac{\pi^2 EI}{L^2}. \tag{8}$$

Figure 2 shows the normalized resonance frequency of a simply supported bimorph with preload increasing from zero to the critical buckling load.

2.3. Piezoelectric device coupling coefficient and preload

The device coupling coefficient k^2 characterizes the effectiveness of electromechanical coupling in a piezoelectric device. In the case of a piezoelectric vibration energy scavenger, the device coupling coefficient is defined as

$$k^2 = \frac{\text{electrical energy recovered}}{\text{mechanical energy supplied}}. \tag{9}$$

Lesieutre and Davis (1997) determined that the device coupling coefficient is affected by preload according to the relationship

$$k^2 = \frac{p^2}{p^2 + (K_o - K_d)C_b} \tag{10}$$

where C_b is the capacitance of the bimorph and p is a piezoelectric coupling term defined as

$$p = 2be_{31}(h_b + h_p)\left(\frac{\pi}{L}\right). \tag{11}$$

Note that in (10), as the preload is increased and K_{app} (equal to $K_o - K_d$) approaches zero, k^2 approaches unity.

Experimentally, the device coupling coefficient can be measured using the expression

$$k_2 = \frac{\omega_o^2 - \omega_c^2}{\omega_o^2} \tag{12}$$

where ω_o and ω_c represent the open-circuit and closed-circuit resonance frequencies of the device, respectively (Roundy and Wright 2004).

It should be noted that the device coupling coefficient discussed here does not include in its calculation the energy required to apply a compressive preload to the piezoelectric generator. The design presented in this paper is intended to operate in 'passive' mode, where the device is tuned by the operator once upon deployment and infrequently thereafter. This scenario does not include any continuous active actuation to tune the device. Thus any energy required to apply this preload is not addressed in this paper.

2.4. Basic piezoelectric generator power model

Williams and Yates (1996) presented a general model for vibration-to-electricity energy conversion. Roundy *et al* (2003) showed that this model can be manipulated to show the following relationship for power output:

$$|\text{Power}| = \frac{m\zeta_e A^2}{4\omega\zeta_T^2}. \tag{13}$$

In this expression, m is the proof mass of the vibration energy scavenger, A is the acceleration magnitude of the driving vibrations, ω is the frequency of the driving vibrations, and ζ_e and ζ_T are the electric and total damping ratios of the energy scavenger, respectively. This relationship also assumes that the resonance frequency of the energy scavenger precisely matches the frequency of the driving vibrations.

The previous equation (13) informs a couple of important guidelines in designing an energy scavenger and selecting a suitable vibration source. In order to maximize power, the designer should use as heavy a proof mass as is feasible. Similarly, in choosing between multiple potential vibration sources, the source with the largest A^2/ω ratio provides the greatest potential for energy scavenging.

A power model for a piezoelectric bimorph vibration energy scavenger was presented by Roundy *et al* (2004), and is shown in (14). This model expresses the power transferred to a resistive load, and it includes the assumption that the driving frequency matches the resonance frequency of the generator.

$$\text{Power} = \frac{1}{\omega^2}\frac{RC_b^2\left(\frac{Y_c d_{31} h_p b^*}{\varepsilon}\right)^2}{\left(4\zeta^2 + k_{31}^4\right)(RC_b\omega)^2 + 4\zeta k_{31}^2(RC_b\omega) + 2\zeta^2} \times A_{in}^2 \tag{14}$$

In this model, ω is the vibration frequency, R is the resistance of the electrical load, C_b is the capacitance of the bimorph,

Y_c is the Young's modulus of the piezoelectric material, d_{31} is the piezoelectric strain coefficient, t_c is the thickness of a single piezoelectric layer, and b^* is a geometric term equal to the ratio of the average strain in a piezo layer to the bimorph's deflection at its center. More precisely, $b^* = 3(h_b + h_p)/L^2$. The dielectric constant of the piezoelectric material is represented by ε, ζ is the damping ratio of the device, k_{31} is the piezoelectric coupling coefficient, and A_{in} is the acceleration magnitude of the driving vibrations.

An optimal load resistance that will maximize power transfer can be determined by differentiating (14) with respect to R, setting the resulting expression equal to zero, and solving for R. The resulting expression for optimal load resistance is

$$R_{opt} = \frac{1}{\omega C_b} \frac{2\zeta}{\sqrt{4\zeta^2 + k_{31}^4}}. \quad (15)$$

This optimal load resistance matches the electrical impedance of the load to that of the generator. It should be noted that the value of R_{opt} has a maximum value of $1/\omega C$. It should further be noted that these models assume that the generator exhibits linear behavior.

3. Experimental apparatus

Each piezoelectric generator used in this research was constructed using a model T220-A4-303X piezoelectric bimorph from Piezo Systems, Inc. The bimorph was comprised of a brass center shim sandwiched between two layers of PZT-5A piezoceramic. A sputtered nickel electrode on the outer surface of each PZT layer allowed for electrical connection. Lead wires were soldered to these outer electrode layers. The PZT layers were poled in series, eliminating the need to connect a lead wire to the center shim. Dimensions and material properties of the bimorph are listed in table 1. A mounting for the proof mass was provided in the form of a flat head screw glued upside-down to the upper surface of the bimorph. Metal bushings were used as proof masses, and were held in place on the screw using small nuts.

A small steel vise was custom-machined to hold the bimorph and facilitate the application of compressive axial preload to tune the resonance frequency of the generator. The vise was designed to be self-centering under preload, with the bimorph held between two sliding L-shaped brackets. Axial preload was applied using a Newport DM-13 differential micrometer drive mounted at one end of the vise. A FlexiForce piezoresistive force sensor from Tekscan, Inc. was mounted at the other end of the vise to measure the applied preload. Figure 3 shows a photograph of the experimental configuration.

The original design incorporated grooved Delrin bushings to hold each end of the bimorph. These bushings were intended to provide a frictionless hinge end condition. Early experimentation showed that these bushings did not provide the desired end condition. A solution to this problem was found by filing the ends of the bimorph to sharp edges, and press-mounting the bimorph between grooves cut into each L-shaped bracket.

A continuously variable resistive load was constructed to measure the generator's output against loads from zero to 375 kΩ. A LabWorks signal amplifier and ET-126 vibrating actuator provided the driving vibrations for the energy scavenger. An Agilent signal generator provided a variable-frequency sine wave signal to the amplifier and vibrometer. Tekscan's ELF software was used to record the output of the force sensors on a notebook computer. A piezoelectric accelerometer from PCB Piezotronics measured the magnitude of the driving vibrations. A two-channel digitizing oscilloscope from Tektronix was used to view and record the output of both the accelerometer and the piezoelectric energy scavenger.

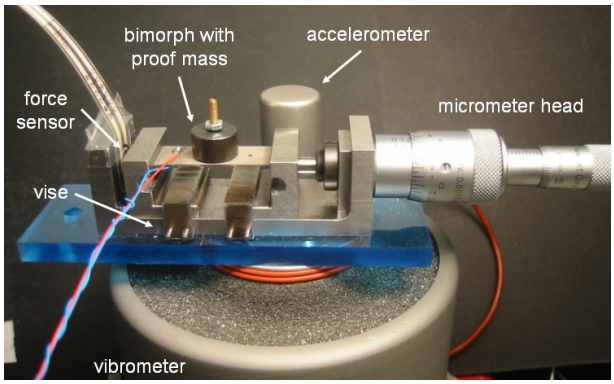

Figure 3. Experimental apparatus.
(This figure is in colour only in the electronic version)

4. Experimental procedure

Experiments were run to study the effects of compressive axial preload on the piezoelectric vibration energy scavengers. Two sets of data were taken using a 7.1 g proof mass and two were taken using a 12.2 g proof mass. The nominal peak acceleration of the driving vibrations used in this experiment was 9.8 m s^{-2}, or approximately 1 g-force. For each data set, a bimorph was mounted in the test apparatus and preload was applied in increments of 8–10 N. The device's resonance characteristics, coupling coefficient, and power output were measured for each level of preload. The preload was increased until the bimorph buckled visibly. After buckling, the bimorph was discarded and not used again for further measurements. It should be noted that the bimorphs buckled well below the critical buckling load predicted by theory. The combination of the proof masses and vibrations likely caused the bimorphs to deform beyond the range in which they were mechanically stable, and they thus buckled.

The open-circuit resonance frequency was measured for each level of preload by varying the frequency of the driving vibrations manually and observing the open-circuit voltage output of the generator using the oscilloscope. Similarly, the closed-circuit resonance frequency was determined using a manual frequency sweep and measuring the voltage drop across a 50 Ω resistor. This resistance was chosen because it was the smallest value that provided a voltage drop large enough to be read on the oscilloscope. The coupling coefficient was calculated from the open-circuit and closed-circuit resonance frequencies using (12).

Power measurements for each level of preload were taken using driving vibrations whose frequency was equal to the

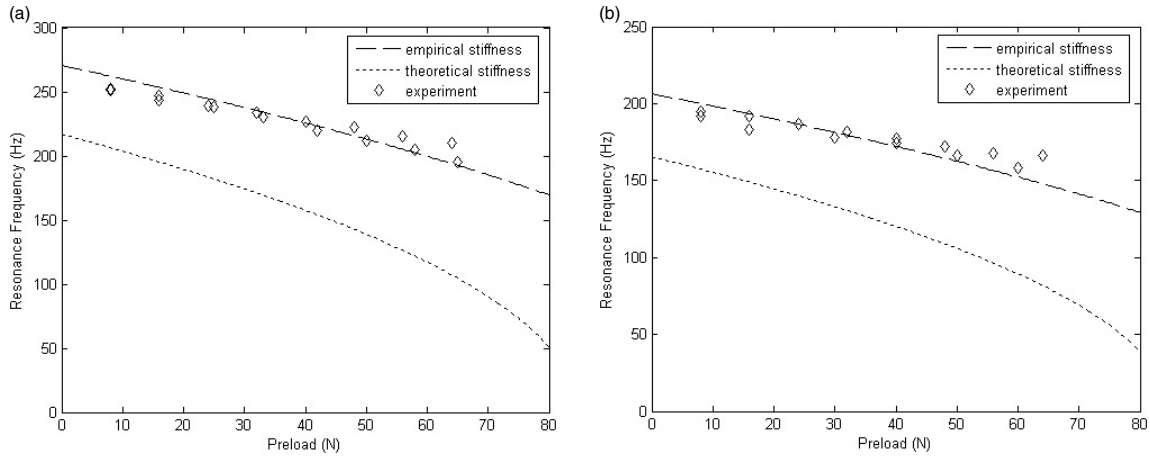

Figure 4. Resonance frequency versus preload, (a) 7.1 g proof mass, (b) 12.2 g proof mass.

open-circuit resonance frequency for that level of preload. The power output was determined by measuring the voltage drop across a known resistance and calculating the power using the relationship $P = V^2/R$. The peak generator power for each level of preload was determined by varying the load resistance in small increments and plotting the results in real time. The maximum power output and corresponding load resistance were noted for each level of preload.

Referring back to (13), it can be seen that the magnitude of the power produced by a vibration energy scavenger is inversely proportional to the frequency of the driving vibrations. As described above, the frequency of the driving vibrations used for power measurements varied as the preload increased. It was thus necessary to compensate for these variations in driving frequency, and ensure properly compared power measurements.

Compensation for these frequency variations was achieved by adjusting the acceleration magnitude of the driving vibrations to achieve an identical A^2/ω ratio across all levels of preload. Referring again to (13), it is seen that in the absence of other variables the power generated by a vibration energy scavenger should be the same using any two vibration sources whose A^2/ω ratios are equal. Consider the following example: the first measurement in a data run found an open-circuit resonance frequency of 250 Hz, and power data were collected using vibrations with a peak acceleration magnitude of 9.8 m s^{-2}. If upon increasing the preload the open-circuit resonance frequency fell to 240 Hz, power measurements for that preload were taken using vibrations with 9.6 m s^{-2} acceleration magnitude in order to maintain a constant A^2/ω ratio between the two power measurements.

The relationship between preload and device damping ratio was also examined experimentally. The bimorph was mounted in its vise and excited with a small mechanical impulse. The decaying oscillatory voltage signal that resulted was recorded using an oscilloscope, and the logarithmic decrement method was used to calculate the damping coefficient. In these experiments, the generator was attached to a 173 kΩ resistive load, a value determined from the power measurements to be near the mean optimal resistance value. These measurements were taken at levels of preload ranging from 0 to 60 N, in 10 N increments.

5. Results and discussion

5.1. Preload and resonance

Figure 4 shows the effects of compressive axial preload on resonance frequency for the piezoelectric generator. Results for generators using proof masses of 7.1 and 12.2 g are shown. For the 7.1 g proof mass, the frequency was reduced from about 250 Hz to just over 200 Hz, a reduction in frequency of about 24%. For the 12.2 g proof mass, the resonance frequency was reduced from just over 190 Hz to 160 Hz, a frequency reduction of about 19%. In both cases, the generator's bimorph failed at loads above 65 N.

In these plots, the dotted line represents the preload–resonance relationship predicted using a theoretical value for the bimorph's transverse stiffness K_o, as determined using (2) and the material constants provided in the bimorph datasheet. The sizeable and consistent discrepancy between this theoretical curve and the experimental results suggests that theory significantly underestimates the actual stiffness of the bimorphs used in this experiment. A number of possible explanations arose to explain this mismatch:

- The ratio of the bimorph's length to its width was only 2.5, whereas beam theory assumes long, slender beams.
- Locally stiff regions of the bimorph existed where the mass-mounting screw was glued on and at the lead wire solder pads.
- As true frictionless pin–pin end conditions are difficult to achieve in practice, the end conditions must have imparted some moment to the beam.

An empirical value for the bimorph's transverse stiffness K_o was calculated from the experimental data. A new preload–resonance curve using this value is plotted as the dashed lines in figure 4. These curves fit the data much more closely, suggesting that the K_o value calculated using beam theory was indeed too low. It should be noted that the curves generated using the empirical K_o are of the same shape as those generated using the theoretical value, differing only in the substitution of the empirical stiffness value into (5) and (7).

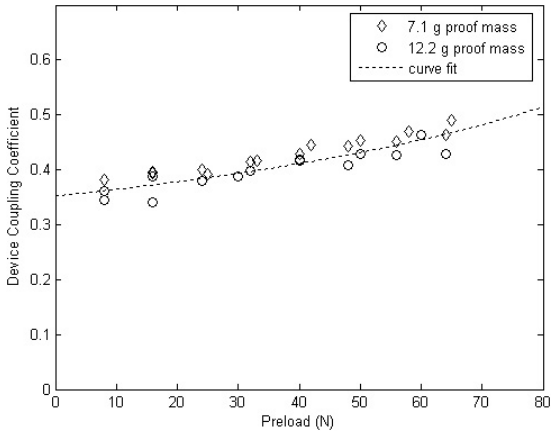

Figure 5. Device coupling coefficient versus preload.

5.2. Preload and coupling coefficient

Figure 5 shows the effect of compressive axial preload on the device coupling coefficient for the piezoelectric generator. The dotted line represents a curve fit using the model described in (10), in which the piezoelectric coupling term p was left as an unknown.

The device coupling coefficient was increased about 25%, from an average of 0.367 with a preload of 8 N to an average of 0.461 with a 64 N preload. The experimental data fit the shape of the curve very well, indicating that the model described in (10) is useful in describing the coupling coefficient behavior. Moreover, the data obtained using a 7.1 g proof mass and those obtained using a 12.2 g proof mass follow one another closely, further illustrating the robustness of this trend.

5.3. Preload and power output

Figure 6 shows the maximum power generated by the device across a range of resonance frequencies. Data are shown for generators using proof masses of 7.1 and 12.2 g. Recall that the resonance frequency of the generator was adjusted downward by increasing the compressive axial preload. The generator using a 7.1 g proof mass output between 300 and 400 μW of power across a range of frequencies from 200 to 250 Hz. The generator using a 12.2 g proof mass showed a larger spread, with power output ranging from 360 to 650 μW over a spread of frequencies between 160 and 195 Hz. These results compare favorably with a fixed-resonance device optimized to run most efficiently when driven at a single specific frequency.

5.4. Preload and device damping

As shown in figure 6, the power output was relatively flat over the range of frequencies examined, even decreasing somewhat at lower frequencies. The relationships described in (13) and (14), however, suggest that the power output should increase at lower frequencies. It was proposed that an increase in device damping at higher levels of preload might explain this decrease in power output. Experiments were thus undertaken to examine the possible relationship between preload and damping ratio. Figure 7(a) shows the effects of preload on both resonance frequency and damping ratio for a generator with a 7.1 g proof mass.

These experiments demonstrated a relationship between preload and device damping ratio, as the damping ratio increased 67% from 0.0265 at 0 N preload to 0.0445 at 60 N preload. Figure 7(b) further shows that the relationship between resonance frequency and damping for a 7.1 g proof mass generator is approximately linear.

5.5. 'Damping-compensated' piezoelectric generator power model

The relationship observed between damping, preload, and resonance frequency suggested that this variability should be accounted for in the theoretical piezoelectric power model described by (14). The linear fit shown in figure 7(b) was thus substituted into the damping term of the power model. The results of this 'damping-compensated' power model are shown in figure 8.

The inclusion of variable damping in the power model results in reasonably accurate predictions of power output

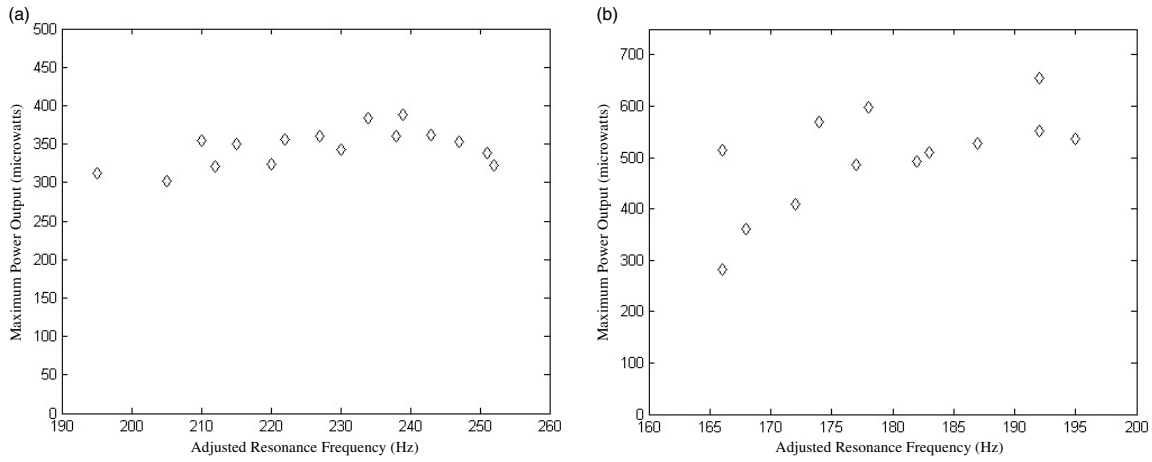

Figure 6. Power output versus resonance frequency, (a) 7.1 g proof mass, (b) 12.2 g proof mass.

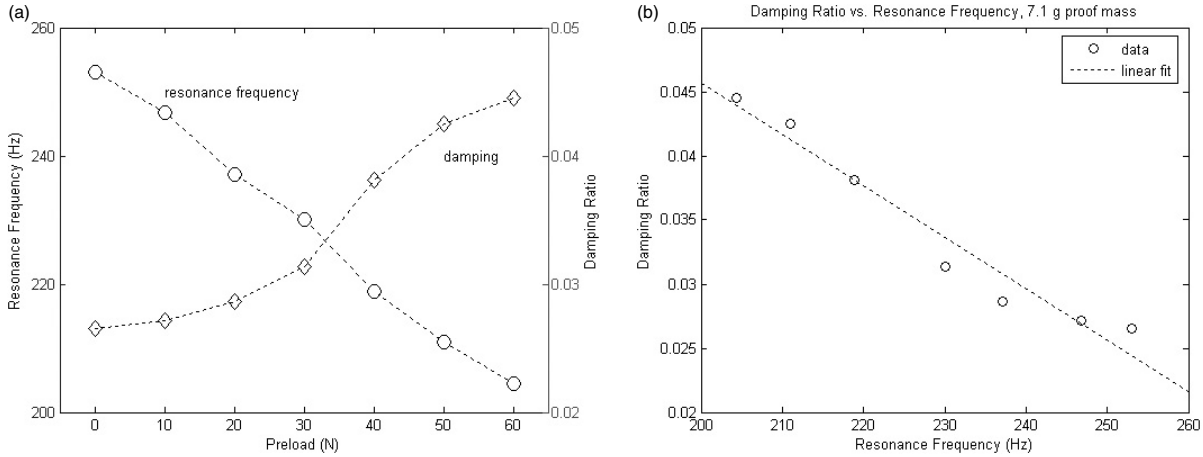

Figure 7. (a) Resonance frequency and damping versus preload, (b) damping versus resonance frequency.

across the range of frequencies observed, though the shape of the curve is less accurate. Further inquiry into the assumptions of the power model may result in better predictions of power output. For example, it may be worthwhile to examine whether the generator's behavior is close to linear, particularly at higher levels of preload. Additionally, while figure 7(b) shows that the relationship between resonance frequency and damping ratio can be approximated as linear, the data suggest that the association may in fact be a more complex S-shaped curve. None of these further inquiries were undertaken in this study, however.

Overall, the power measurements presented here are highly encouraging. Using a compressive axial preload it is clearly possible to construct a tunable-resonance vibration energy scavenger that can produce significant power across a range of driving frequencies. These experiments indicate that this method of resonance tuning can allow a single energy scavenging device to work in a variety of different environments.

5.6. Optimal load resistance

Each power measurement presented in the previous section corresponds to an optimal load resistance determined according to the method described in section 4. Figure 9(a) shows a single set of power versus resistance data and is presented as an illustrative example. Figure 9(b) shows all optimal load resistance values plotted with their associated resonance frequencies. The curve on the plot represents the optimal resistance values predicted by the piezoelectric power model and was generated using (15).

It is immediately apparent that the optimal load resistance values observed experimentally are larger than the values predicted by the piezoelectric power model by a factor of three to four. A partial explanation for this discrepancy may lie in the way in which the proof mass was mounted to the bimorph. The proof mass was mounted on a small flathead screw glued to the center of the bimorph's upper surface. This mounting resulted in a locally stiff 4.5 mm diameter circle at the center of the bimorph, precisely where the strain (and thus the charge separation) would otherwise have been largest. This effect may have raised the apparent impedance of the generator, though it is unlikely that it would sufficiently explain a difference of the magnitude shown in figure 9(b). The optimal load resistance behavior of these generators merits further investigation.

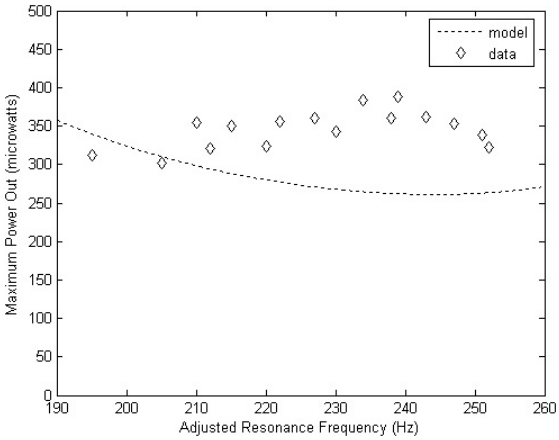

Figure 8. Power output versus resonance frequency, theory and experiment.

6. Conclusions and future work

(1) This paper presents research undertaken to examine the effects of compressive axial preload on a vibration energy scavenger build around a piezoelectric bimorph. In particular, this study sought to evaluate the potential of this technique to enable an energy scavenger to work effectively in a variety of environments with ambient vibrations of different frequencies.

(2) It was determined that a compressive axial preload can reduce the resonance frequency of a vibration energy scavenger up to 24% while increasing the device coupling coefficient up to 25%. Most importantly, the experimental data presented herein show that a single energy scavenging device can be tuned to produce significant power across a range of frequencies. A generator using a 7.1 g proof mass was shown to produce 300–400 μW of power while

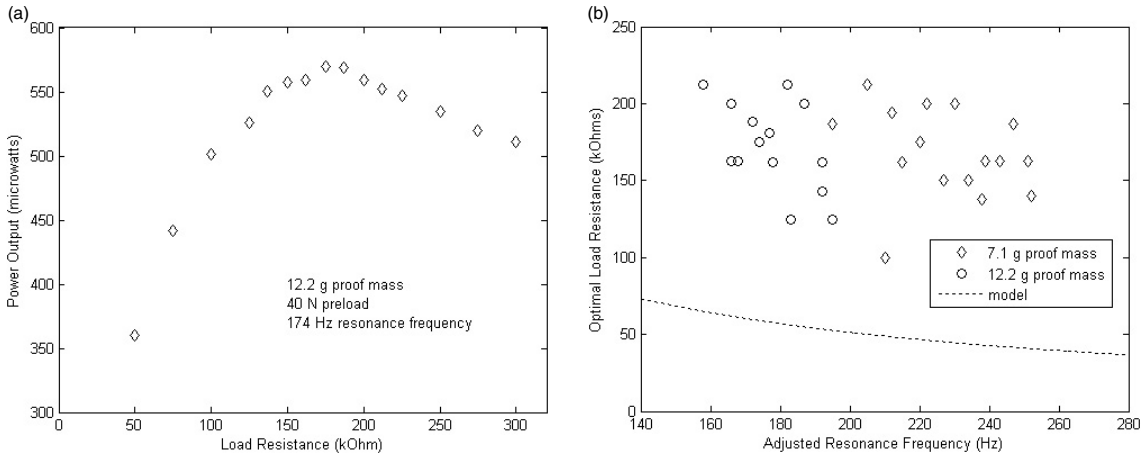

Figure 9. (a) Power output versus load resistance, (b) load resistance versus resonance frequency.

operating across the range of 200–250 Hz. Similarly, a generator using a 12.2 g proof mass produced between 360 and 650 μW of power across a range of frequencies from 165 to 190 Hz. These results suggest that a compressive axial preload presents a viable option for building vibration energy scavengers that can be tuned to operate effectively in a variety of different application settings.

(3) Several different avenues for future inquiry were suggested in the course of this study. While the piezoelectric power model used in this project provided reasonable predictions for device power output, the shape of the power curve generated by the model differs from that suggested by the experimental data. The power model's assumption of linear behavior should be evaluated, as should the relationship between preload and damping. The large discrepancy between predicted and observed optimal resistance values was not adequately explained and should be examined further. From a design perspective, a few possible improvements are immediately apparent. The bimorph's end conditions could be modified to more closely resemble a frictionless hinge mount. The proof mass mounting can be improved to eliminate the locally stiff region at the bimorph's center which would otherwise contribute significantly to power generation. These areas of future analytical and design work could play a major role in the development of commercially viable tunable resonance vibration energy scavengers.

(4) Further future work may also include combining this design for a tunable-resonance energy scavenger with an actuator and closed-loop controller. The resulting 'smart scavenger' could periodically seek the level of preload that corresponds to the most efficient resonance frequency for power generation.

Acknowledgments

The authors would like to thank the California Energy Commission for supporting this research under award DR-03-01, as well as the ASEE/NDSEG graduate research fellowship program. Many thanks also to Dr Shad Roundy and Jessy Baker for their help and guidance.

References

Baker J, Roundy S and Wright P 2005 Alternative geometries for increasing power density in vibration energy scavenging for wireless sensor networks *3rd Int. Energy Conversion Engineering Conf. (San Francisco, CA, August 2005)*

Glynne-Jones P, Beeby S P and White N M 2001 Towards a piezoelectric vibration-powered microgenerator *IEE Proc.* A **148** 68–72

Glynne-Jones P, Tudor M J, Beeby S P and White N M 2004 An electromagnetic, vibration-powered generator for intelligent sensor systems *Sensors Actuators* A **110** 344–9

James E P, Tudor M J, Beeby S P, Harris N R, Glynne-Jones P, Ross J N and White N M 2004 An investigation of self-powered systems for condition monitoring applications *Sensors Actuators* A **110** 171–6

Leland E S, Lai E M and Wright P K 2004 A self-powered wireless sensor for indoor environmental monitoring *WNCG 2004 Wireless Networking Symp. (Austin, TX, Oct. 2004)*

Lesieutre G A and Davis C L 1997 Can a coupling coefficient of a piezoelectric actuator be higher than those of its active material? *J. Intell. Mater. Syst. Struct.* **8** 859–67

Miyazaki M, Tanaka H, Ono G, Nagano T, Ohkubo N, Kawahara T and Yano K 2003 Electric-energy generation using variable-capacitative resonator for power-free LSI: efficiency analysis and fundamental experiment *ISPLED 2003 (Seoul, Korea, August 2003)*

Roundy S, Leland E S, Baker J, Carleton E, Reilly E, Lai E, Otis B, Rabaey J M, Wright P K and Sundararajan V 2005 Improving power output for vibration-based energy scavengers *IEEE Pervasive Computing* **4** 28–36

Roundy S and Wright P K 2004 A piezoelectric vibration based generator for wireless electronics *Smart Mater. Struct.* **13** 1131–42

Roundy S, Wright P K and Rabaey J 2003 A study of low level vibrations as a power source for wireless sensor nodes *Comput. Commun.* **26** 1131–44

Roundy S, Wright P K and Rabaey J 2004 *Energy Scavenging for Wireless Sensor Networks with Special Focus on Vibrations* (Boston, MA: Kluwer–Academic) ISBN 1-4020-7663-0

Roundy S and Zhang Y 2005 Toward self-tuning adaptive vibration based micro-generators *Proc. SPIE* **5649** 373–84

Williams C B and Yates R B 1996 Analysis of a micro-electric generator for microsystems *Sensors Actuators* A **52** 8–11